

# Presynaptic $\text{Ca}^{2+}$ Requirements and Developmental Regulation of Posttetanic Potentiation at the Calyx of Held

Natalya Korogod, Xuelin Lou, and Ralf Schneggenburger

AG Synaptische Dynamik und Modulation and Abteilung Membranbiophysik, Max-Planck-Institut für Biophysikalische Chemie, D-37077 Göttingen, Germany

Large excitatory synapses in the auditory system, such as the calyx of Held, faithfully transmit trains of action potentials up to a frequency of a few hundred hertz, and these synapses are thought to display a limited repertoire of synaptic plasticity. Here, we show that brief trains of 100 Hz stimulation induce posttetanic potentiation (PTP) of transmitter release at the calyx of Held. In young rats [postnatal day 4 (P4) to P6], PTP could be induced with shorter 100 Hz trains compared with older age groups (P8–P10 and P12–P14), but the maximal amount of PTP was similar, with  $\sim 200\%$  of control EPSC amplitude. The size of the readily releasable pool of vesicles was not increased significantly during PTP. Bath application of the membrane-permeable  $\text{Ca}^{2+}$  chelator EGTA-AM suppressed PTP, indicating a role for presynaptic  $\text{Ca}^{2+}$  in PTP at the calyx of Held. Presynaptic  $\text{Ca}^{2+}$  imaging showed that the intracellular  $\text{Ca}^{2+}$  concentration,  $[\text{Ca}^{2+}]_i$ , was increased by 40–120 nM at the peak of PTP, and this “residual”  $[\text{Ca}^{2+}]_i$  decayed in parallel with PTP, with time constants in the range of 10–60 s. During whole-cell recording of the presynaptic calyx of Held, PTP was absent, and the decay of residual  $[\text{Ca}^{2+}]_i$  was strongly accelerated. The data show that the calyx of Held expresses a mechanism of transmitter release potentiation in which a small, sustained elevation of basal  $[\text{Ca}^{2+}]_i$  increases the transmitter release probability after trains of high-frequency stimulation.

**Key words:** synaptic plasticity; nerve terminal; transmitter release; release probability; calcium; imaging

## Introduction

The calyx of Held is a large glutamatergic excitatory synapse in the auditory brainstem pathway, formed between an axon of a globular bushy cell in the anterior ventral cochlear nucleus and a principal cell of the contralateral medial nucleus of the trapezoid body (MNTB) (Harrison and Irving, 1966; Friauf and Ostwald, 1988; Spirou et al., 1990; Kuwabara et al., 1991). The calyx of Held contains several hundred active zones (Sätzler et al., 2002; Taschenberger et al., 2002), a morphological specialization that allows this synapse to produce large, multiquantal EPSCs, which reliably and rapidly drive the postsynaptic principal cell to the threshold for action potential (AP) firing. Thus, the function of the calyx of Held synapse is generally regarded as that of a fast relay synapse in the neuronal circuits of the auditory brainstem that processes sound-source localization.

During repetitive activity, EPSCs at the calyx of Held undergo strong, frequency-dependent depression (Borst et al., 1995; von Gersdorff et al., 1997; Wang and Kaczmarek, 1998), which is mediated both by presynaptic and postsynaptic mechanisms (Schneggenburger et al., 1999; Wu and Borst, 1999; Neher and Sakaba, 2001; Scheuss et al., 2002; Wong et al., 2003). The finding

that depression is the prevalent form of short-term plasticity has initially led to the view that the release probability at this synapse must be quite high (Chuhma and Ohmori, 1998; Weis et al., 1999). Evidence has accumulated, however, that a presynaptic AP releases a surprisingly small fraction of the pool of readily releasable vesicles. For example, it has been shown that increasing the external  $\text{Ca}^{2+}$  concentration leads to a pronounced, approximately fivefold increase of the EPSC amplitude at the calyx of Held (Schneggenburger et al., 1999; Iwasaki and Takahashi, 2001; Meyer et al., 2001). Also, strong direct stimulation of the calyx of Held by voltage clamp or  $\text{Ca}^{2+}$  uncaging has revealed a large pool of readily releasable vesicles (RRP) (Schneggenburger and Neher, 2000; Sakaba and Neher, 2001; Sun and Wu, 2001), implying, again, that the fraction of the RRP released by a single presynaptic AP must be quite small. This small release fraction is a property shared with other CNS synapses (Reim et al., 2001; Hallermann et al., 2003) and indicates that potentiation of transmitter release might occur under certain physiological conditions.

Here, we show that brief trains of 100 Hz stimuli induce a robust form of short-term potentiation at the calyx of Held, which shares many properties with posttetanic potentiation (PTP) studied previously at hippocampal synapses and at neuromuscular junctions. We find a developmental regulation of PTP, with an increased sensitivity for PTP induction early postnatally [postnatal day 4 (P4) to P6] compared with later developmental stages. During PTP, a surprisingly small elevation of presynaptic  $[\text{Ca}^{2+}]_i$  by  $\sim 80$  nM induces a robust, approximately twofold potentiation of release probability. Whole-cell recording of the presynaptic nerve terminal abolished PTP because of an accelerated decay of residual  $[\text{Ca}^{2+}]_i$ , explaining why PTP has not been ob-

Received July 22, 2004; revised April 14, 2005; accepted April 14, 2005.

This work was supported by grants from the Deutsche Forschungsgemeinschaft (Schn 451/4-1 and SFB-406) and a Heisenberg fellowship to R.S. We thank Erwin Neher, Takeshi Sakaba, Holger Taschenberger, and Sam Young for helpful discussions and for comments on this manuscript.

Correspondence should be addressed to Dr. Ralf Schneggenburger, AG Synaptische Dynamik und Modulation and Abteilung Membranbiophysik, Max-Planck-Institut für Biophysikalische Chemie, Am Fassberg 11, D-37077 Göttingen, Germany. E-mail: rschne@gwdg.de.

DOI:10.1523/JNEUROSCI.1295-05.2005

Copyright © 2005 Society for Neuroscience 0270-6474/05/255127-11\$15.00/0

served in previous studies with paired presynaptic and postsynaptic recordings (Forsythe et al., 1998).

## Materials and Methods

**Electrophysiology and slice preparation.** Transverse 200- $\mu\text{m}$ -thick brainstem slices containing the MNTB were made with a vibratome slicer (Integralslice 7550 MM; Campden Instruments, Leicester, UK) using Wistar rats at P4–P14, with P0 referring to the day of birth. Slices were kept at 36°C in a bicarbonate-buffered solution composed of the following (in mM): 125 NaCl, 25 NaHCO<sub>3</sub>, 1.25 NaH<sub>2</sub>PO<sub>4</sub>, 2.5 KCl, 2 CaCl<sub>2</sub>, 1 MgCl<sub>2</sub>, 25 glucose, 3 *myo*-inositol, 2 Na-pyruvate, 0.4 ascorbic acid, pH 7.4 when bubbled with 95% O<sub>2</sub>/5% CO<sub>2</sub>. One slice at a time was transferred after a minimum of 30 min to the experimental chamber in an upright microscope (Olympus, Hamburg, Germany) equipped with infrared gradient contrast illumination (Luigs and Neumann, Ratingen, Germany). During recordings, the bicarbonate-buffered solution (see above) was used as the standard perfusion solution. For the experiments in Figures 1 and 6, 1  $\mu\text{M}$  strychnine and 10  $\mu\text{M}$  bicuculline were present in the extracellular solution, and in some experiments shown in Figure 4, 1 mM kynurenic acid (KYN) and 0.1 mM cyclothiazide (CTZ) were used. Postsynaptic recordings were made in the voltage-clamp mode at a holding potential of  $-70$  mV. Series resistance ( $R_s$ ; range, 4–15 M $\Omega$ ) was compensated up to 80%, such that the uncompensated  $R_s$  never exceeded 3 M $\Omega$ . EPSC traces were corrected off-line for the remaining  $R_s$  error (Meyer et al., 2001). Presynaptic recordings (see Fig. 8) were done under current clamp, and the membrane potential before afferent fiber stimulation was kept close to  $-70$  mV by injecting a constant, small (range,  $-60$  to  $+30$  pA) holding current. Recordings were made at room temperature (22–25°C) with an EPC-9/2 patch-clamp amplifier (HEKA, Lambrecht, Germany).

EPSCs were evoked by stimulating presynaptic axons with a concentric, bipolar stimulating electrode (MCE-100; Rhodes Medical Instruments, Woodland Hills, CA), placed between the medial border of the MNTB and the midline of the brainstem. With this stimulation method, suitable postsynaptic cells ( $\sim 10$ – $30\%$  of superficial cells) were selected by measuring the presynaptic and postsynaptic action currents after afferent fiber stimulation (Borst et al., 1995; Meyer et al., 2001). In some experiments, afferent fibers were stimulated by a monopolar stimulation electrode mounted inside a wide-opening (5–10  $\mu\text{m}$ ) patch pipette, placed in the vicinity ( $\sim 20$ – $50$   $\mu\text{m}$ ) of a recorded MNTB principal cell. With both methods, we found robust PTP after 100 Hz stimulation trains. Postsynaptic patch pipettes contained the following (in mM): 140 Cs-gluconate, 20 tetraethylammonium-Cl, 10 HEPES, 5 EGTA, 4 Mg-ATP, 0.3 Na-GTP, and 5 Na<sub>2</sub>-phosphocreatine, pH 7.2. The pipette solution for presynaptic whole-cell recordings contained the following (in mM): 140 K-gluconate, 20 KCl, 10 HEPES, 4 Mg-ATP, 0.3 Na-GTP, and 5 Na<sub>2</sub>-phosphocreatine, pH 7.2.

Baseline synaptic strength was evaluated by paired (10 ms interval) afferent fiber stimuli, repeated every 10 s. During the intervening intervals, 9.6 s stretches of postsynaptic current were recorded (sampling frequency, 20 kHz; low-pass filter, 6 kHz) to evaluate the amplitude and frequency of spontaneous miniature EPSCs (mEPSCs). The mEPSCs were detected off-line with a template-matching routine (Clements and Bekkers, 1997). Amplitude histograms of mEPSCs (see Fig. 1E) were constructed for control conditions and for short time periods ( $<30$  s) after the induction of PTP. For the plot of Figure 6E, the average mEPSC frequency was calculated for each 9.6 s sampling interval.

**[Ca<sup>2+</sup>]<sub>i</sub> imaging.** To preload the calyx with Ca<sup>2+</sup> indicator (see Fig. 6), we made a brief (1–2 min) presynaptic whole-cell recording with the K-gluconate-containing pipette solution given above, to which 200  $\mu\text{M}$  fura-4F was added. We estimate that this procedure resulted in the loading of calyces with 80–120  $\mu\text{M}$  fura-4F, based on the fluorescence intensity of calyces measured during longer-lasting presynaptic whole-cell recordings with 100  $\mu\text{M}$  fura-4F. [Ca<sup>2+</sup>]<sub>i</sub> imaging was done using a monochromator (TILL Photonics, Gräfelting, Germany) to excite fura-4F at 350 and 380 nm. A slow-scan CCD camera (TILL Photonics) using on-chip binning (8 × 15 pixels) and 10 ms exposure times imaged the resulting fura-4F fluorescence signals. Pairs of images at each wavelength were taken at 0.5 Hz before and after the induction of PTP and at

20 Hz during 100 Hz trains. [Ca<sup>2+</sup>]<sub>i</sub> was calculated from background-corrected fluorescence values collected from the six to eight brightest superpixels located in the calyx area (see Fig. 6A, bottom panel), using the equation given by Grynkiewicz et al. (1985). The calibration constants were determined in a calibration procedure (Felmy et al., 2003) that combines *in vitro* measurements in thin quartz-glass capillaries and *in-cell* measurements of the limiting ratios at low [Ca<sup>2+</sup>]<sub>i</sub> and at a suitable intermediate [Ca<sup>2+</sup>]<sub>i</sub> (1.04  $\mu\text{M}$  for fura-4F).

**Data analysis.** Data analysis was done in IgorPro (WaveMetrics, Lake Oswego, OR). PTP was standardly expressed as the relative EPSC amplitude at the time of peak PTP, according to the following:  $\text{PTP} = (\text{EPSC}_{\text{PTP}}/\text{EPSC}_{\text{control}}) \times 100$ . This corresponds to the following relationship:  $\text{PTP} = (p/b) \times 100$  (see Fig. 5B). For the plot of Figure 5D, the absolute increment of EPSC amplitude during the peak of PTP was analyzed, corresponding to the amplitude value  $i$  in Figure 5B.

The control EPSC amplitude was determined individually for each PTP induction, by averaging the second (or sometimes third) up to the fifth EPSC preceding the 100 Hz train. The first one or two EPSCs were not included in the control average, because these EPSCs were often larger than the subsequent ones, indicating that some depression occurred even at the low frequency (0.1 Hz) with which the control EPSCs were elicited (von Gersdorff et al., 1997).

The decay times of PTP and residual [Ca<sup>2+</sup>]<sub>i</sub> were estimated by fits with single-exponential functions. For these fits, the baseline values were constrained to the average of the last three or four data points in each series. Average data are reported as mean  $\pm$  SEM, with the exception of the plots in Figures 3D and 7C, which show mean  $\pm$  SD values. Statistical significance was evaluated with Student's *t* test, unless noted otherwise.

## Results

### Identification of posttetanic potentiation at the calyx of Held

Figure 1A–C shows an experiment designed to test whether brief trains of 100 Hz stimulation induce posttetanic potentiation at the calyx of Held. We first assessed baseline synaptic strength with double stimuli (interstimulus interval, 10 ms), repeated five times every 10 s (Fig. 1A). Subsequently, a 100 Hz train of 4 s duration was applied (Fig. 1B), and double stimuli were resumed at 0.1 Hz, to probe the development of synaptic strength (Fig. 1C).

During the 100 Hz train, EPSCs strongly depressed (Fig. 1B, top). The EPSC amplitudes at the end of the 100 Hz train were depressed to  $2.8 \pm 0.8\%$  ( $n = 6$  cells) of the control EPSC amplitude. The earliest EPSCs after the 100 Hz train, corresponding to the light gray traces in Figure 1C, were still depressed, but later EPSCs recovered from depression and then showed a marked, approximately twofold overshoot in amplitude at  $\sim 20$ – $30$  s after the 100 Hz train. Thereafter, synaptic strength returned to baseline over the next 8–10 stimuli. Figure 1D shows the corresponding plot of the first and second EPSC amplitude before and after the 100 Hz train. The transient potentiation of the first EPSC amplitude is reminiscent of PTP, which has been described at the neuromuscular junction (Magleby and Zengel, 1975), at crayfish neuromuscular synapses (Delaney et al., 1989), and at hippocampal synapses (McNaughton, 1982; Griffith, 1990).

During the peak of PTP, the first EPSC was potentiated to  $202 \pm 31\%$  of the baseline value ( $n = 8$  cells; 4 s induction train; P4–P6), whereas the second EPSC, at the time of the maximal potentiation of the first EPSC, was decreased to  $73 \pm 11\%$  of its corresponding control value ( $n = 8$  cells) (Fig. 1D, H). Thus, the paired-pulse ratio (EPSC2/EPSC1) was decreased at the peak of the EPSC potentiation (Fig. 1I), indicative of a presynaptic mechanism for PTP. Additional support for a presynaptic mechanism is given by the observation that immediately after the 100 Hz train, the frequency of mEPSCs was strongly increased (Fig. 1B, middle, G), whereas the amplitude distributions of mEPSCs were unchanged (Fig. 1E, F). In addition, the finding that PTP was

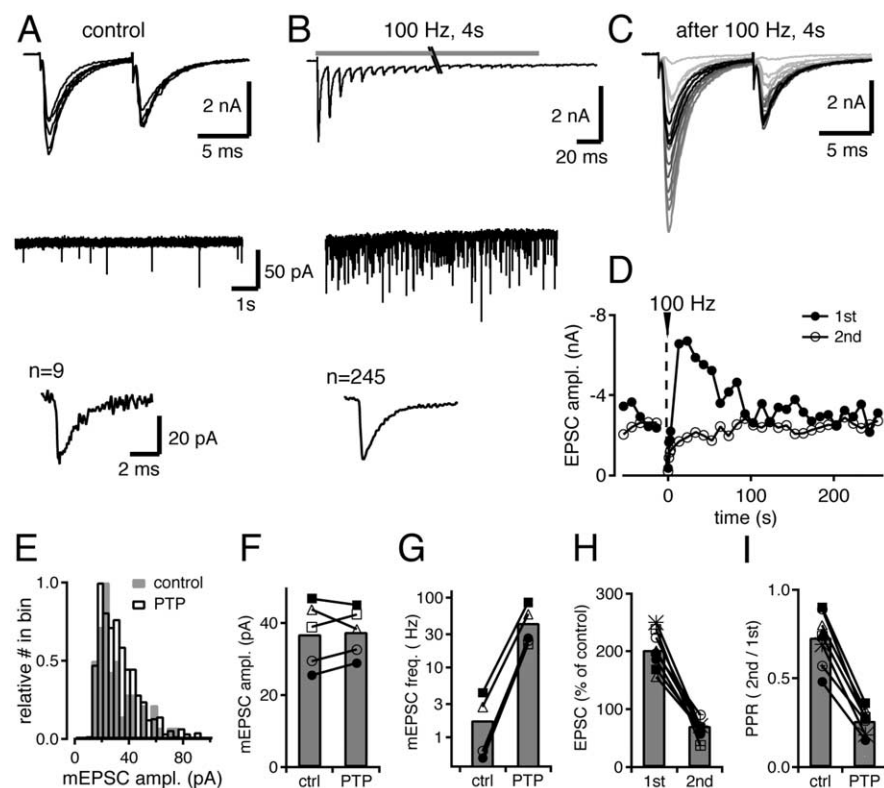


**Figure 1.** Posttetanic potentiation at the calyx of Held. **A**, Top, EPSCs in response to a pair of fiber stimulations separated by 10 ms, repeated every 10 s. The middle panel shows a 9.6 s stretch of postsynaptic current, and the bottom panel shows the average trace of  $n = 9$  detected mEPSCs. **B**, EPSC in response to a 4 s, 100 Hz train of afferent fiber stimulation, applied 10 s after the last control EPSC shown in **A**. Only the first and the last 10 EPSCs in the train are shown, and the stimulation artifacts have been blanked for clarity. The middle panel shows a postsynaptic current record, starting 3.7 s after the end of the 100 Hz train. Note the strongly increased frequency of mEPSCs throughout the entire record. The bottom panel shows the average trace of all detected mEPSCs from this sweep ( $n = 245$ ). **C**, EPSCs in response to a pair of stimuli repeated every 10 s after the 100 Hz train. The traces are grayscale coded, with the earliest traces after the 100 Hz train shown in light gray. **D**, Time course of EPSC amplitudes for the experiment shown in **A–C**. Filled and open circles represent amplitudes of the first and second EPSC, respectively. Note the transient overshoot of the first EPSC amplitude. **E**, mEPSC amplitude distribution for the control period (hatched bars) and for a period of 30 s after the 100 Hz train (open bars), corresponding to the time of development of maximal PTP. The mean mEPSC amplitudes were 30 and 33 pA for control and PTP, respectively. The data in **A–E** are from a recording in a P7 rat. **F**, Mean of the mEPSC amplitude distributions, plotted for individual cells for control conditions and after induction of PTP. **G**, Mean mEPSC frequencies (freq.) derived from individual cells before and after PTP induction. Note the strong increase in mEPSC frequency after the 100 Hz train. **H**, Maximal potentiation of the first and second EPSC amplitude for  $n = 8$  cells. **I**, Paired-pulse ratio (EPSC2/EPSC1) for the control period and during maximal potentiation of the EPSCs. The data shown in **F–I** were obtained from recordings in P4–P7 rats. ampl., Amplitude; ctrl, control.

absent during whole-cell recording of a presynaptic calyx (see below, Fig. 8) also indicates that PTP at the calyx of Held has a presynaptic origin, similar to that at other synapses (Zucker and Regehr, 2002).

We next investigated how the amplitude and the time course of PTP depended on the duration of the induction trains (Fig. 2). PTP was induced repetitively in a given cell, with varying lengths of the 100 Hz trains. We found that the amplitude, as well as the duration of PTP, increased after prolonging the 100 Hz induction trains. In the example of Figure 2A, a short 100 Hz train of 0.2 s duration induced noticeable PTP of 150% of control, which, on average, was  $136 \pm 6.6\%$  for the age group of P4–P6 ( $n = 10$  cells) (Fig. 2B). Prolonging the 100 Hz induction trains led to larger PTP with slowed decay time constants (Fig. 2B,C). When the length of the induction trains was prolonged beyond 1 s, the amplitude of PTP was not further increased ( $p > 0.5$  for all pairwise comparisons between 2, 4, and 8 s trains), suggesting that PTP was maximal for induction trains of 2 s or longer.

**Developmental regulation of posttetanic potentiation**

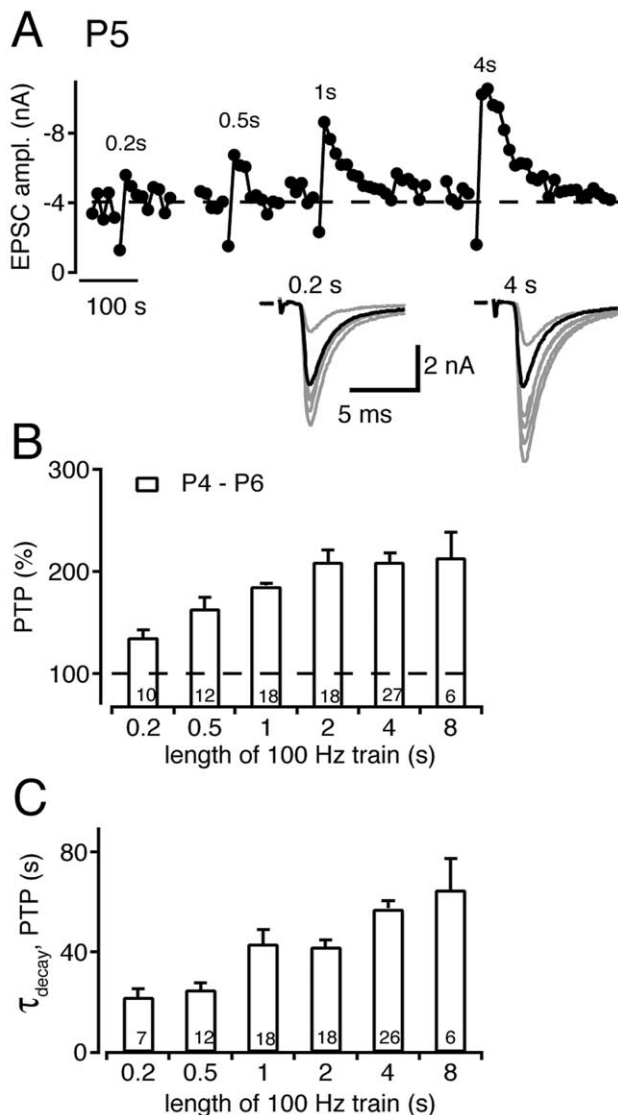
The data presented in Figures 1 and 2 was obtained from calyx of Held synapses from young rats (P4–P6). It is known, however, that the functional properties of transmission at the calyx of Held undergo pronounced developmental changes before and after the onset of hearing around P12 in rodents (Taschenberger and von Gersdorff, 2000; Iwasaki and Takahashi, 2001; Joshi and Wang, 2002). To investigate whether the properties of PTP might change during postnatal development, we studied PTP in two older age groups, at P8–P10 and at P12–P14 (Fig. 3). At these later developmental stages, we also observed PTP, but longer induction trains were needed to obtain PTP with similar amplitudes as in younger animals. In the example of Figure 3A, a recording from a P13 animal is shown. Note that 100 Hz trains with 0.5 and 1 s durations did not induce noticeable PTP in this cell, but PTP was induced by longer induction trains.

Figure 3B plots the average PTP amplitude as a function of the length of the induction train for all three age groups investigated here. In the older age groups (P8–P10 and P12–P14), PTP in response to the short trains was significantly smaller compared with PTP at P4–P6 ( $0.2–2$  s;  $p < 0.01$  or  $0.001$ ) (Fig. 3B). With 100 Hz induction trains of 4 and 8 s, however, PTP was not significantly different between the age groups ( $p > 0.5$  for all comparisons). Thus, the maximal amount of PTP was not changed during development, but longer 100 Hz trains were needed in the older animals to induce a given amount of PTP. This data show that the threshold for PTP induction is lower for synapses at P4–P6 compared with the older age groups investigated here (P8–P10 and P12–P14).

In Figure 3C, we plotted the amplitude of PTP in response to 4 s induction trains (or 2 s in some cases) as a function of the control EPSC amplitude in each cell. We found that PTP tended to be smaller in cells with large control EPSC amplitudes, indicating that some presynaptic or postsynaptic resource might become limiting for the full expression of PTP, when the initial EPSC amplitude is large. In agreement with previous findings (Taschenberger and von Gersdorff, 2000), we found that the average EPSC amplitudes were not different between P4 and P14 ( $p > 0.1$ ), although the EPSC amplitudes showed a quite large scatter between individual cells (Fig. 3D). In the following experiments, we investigated the properties of PTP at young calyces of Held (P4–P6), except for the results in Figure 8, in which P8–P10 rats were used.

**PTP is mediated by an increased release probability**

Based on the constant mEPSC amplitudes after 100 Hz induction trains (Fig. 1B,F), PTP was presynaptic in origin, similar as at other synapses (Zucker and Regehr, 2002). We next tested



**Figure 2.** Dependence of PTP amplitude and duration on the length of 100 Hz induction trains. **A**, An experiment at P5, in which the PTP protocol shown in Figure 1 was applied several times. The length of the 100 Hz induction trains is indicated. The traces at the bottom are the averaged control EPSCs before induction (black trace;  $n = 5$ ) and the first 10 EPSCs after the induction of PTP. **B**, Amplitude of PTP as a function of the length of the 100 Hz induction train for the age group of P4–P6. The number of cells investigated is indicated for each bar. **C**, Dependence of the decay time constant of PTP, estimated from fitting the decay phase of PTP with single-exponential functions, as a function of the length of the 100 Hz induction train. Error bars represent SEM.

whether an increased size of a pool of immediately available vesicles contributed to the presynaptic mechanism of PTP (Fig. 4). To do so, we used a method in which the EPSC amplitude plots in response to 100 Hz trains is analyzed (Schneppenburger et al., 1999). The cumulative EPSC amplitude plots in response to 100 Hz trains were fitted with a line, and the back-extrapolated EPSC amplitude value at time 0 was taken as a measure of the pool size (Fig. 4A).

In these experiments, PTP was induced by a 4 s 100 Hz train, and the pool size for control conditions was estimated by analyzing the first 25 EPSCs of the first induction train (Fig. 4A, black trace and black symbols). When PTP was maximal at  $\sim 20$ – $30$  s after the first 100 Hz train, a second 100 Hz train with 4 s duration was applied to test whether the pool size was increased (Fig. 4B,

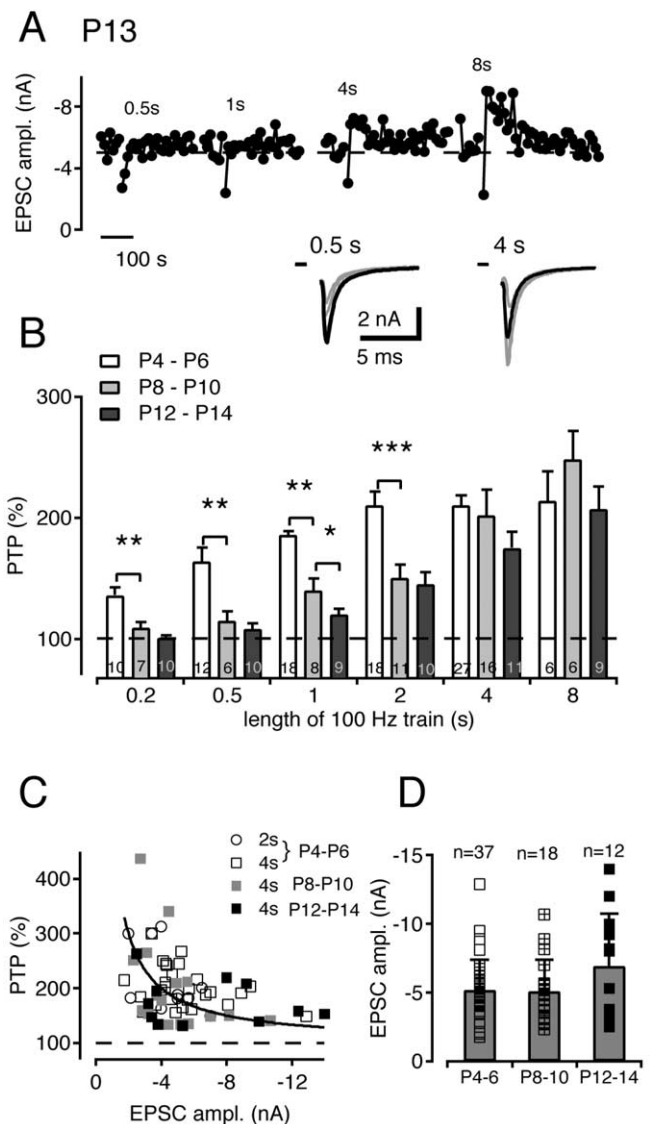


**Figure 3.** Developmental regulation of PTP at the calyx of Held. **A**, An experiment at P13, in which PTP was induced with 100 Hz trains of indicated lengths. Note that the shorter 100 Hz trains (0.5 s, 1 s) did not induce notable PTP in this cell. The inset shows sample traces for the 0.5 and 4 s induction trains. **B**, Amplitude of PTP as a function of the length of the 100 Hz induction train, separated for the age groups of P4–P6 (open bars; replotted from Fig. 2B), P8–P10 (gray bars), and P12–P14 (black bars). Note that the short 100 Hz trains of 0.2–2 s induced significantly larger PTP at P4–P6 than in the older age groups. Asterisks indicate a significant difference between the indicated pairwise comparisons ( $*p < 0.05$ ;  $**p < 0.01$ ;  $***p < 0.001$ ; unpaired  $t$  test). Error bars represent SEM. **C**, Scatter plot of PTP amplitude as a function of the control EPSC amplitude. For the data obtained at P4–P6, results from 2 and 4 s induction trains are shown, whereas in the older age groups, only 4 s induction trains were analyzed, with the meaning of each symbol as indicated. The data set was fitted by an inverse function. Note the tendency toward smaller PTP for initially large EPSCs. **D**, Plot of average control EPSC amplitudes from individual cells for each age group. The average  $\pm$  SD of each data set is shown superimposed. **Ampl.**, Amplitude.

second arrow). At the peak of PTP, the pool size was increased to  $107 \pm 2\%$  of its control value ( $n = 6$  cells). This small increase in pool size can account only for a small fraction ( $< 10\%$ ) of the overall amount of PTP, which was  $221 \pm 13\%$  in these experiments ( $n = 6$ ). This can also be seen in Figure 4C, which plots the relative increase of pool size as a function of the PTP for each cell. Note that the data points lie far below the unity line that is indicated by the dashed line. To reduce possible influences of AMPA-

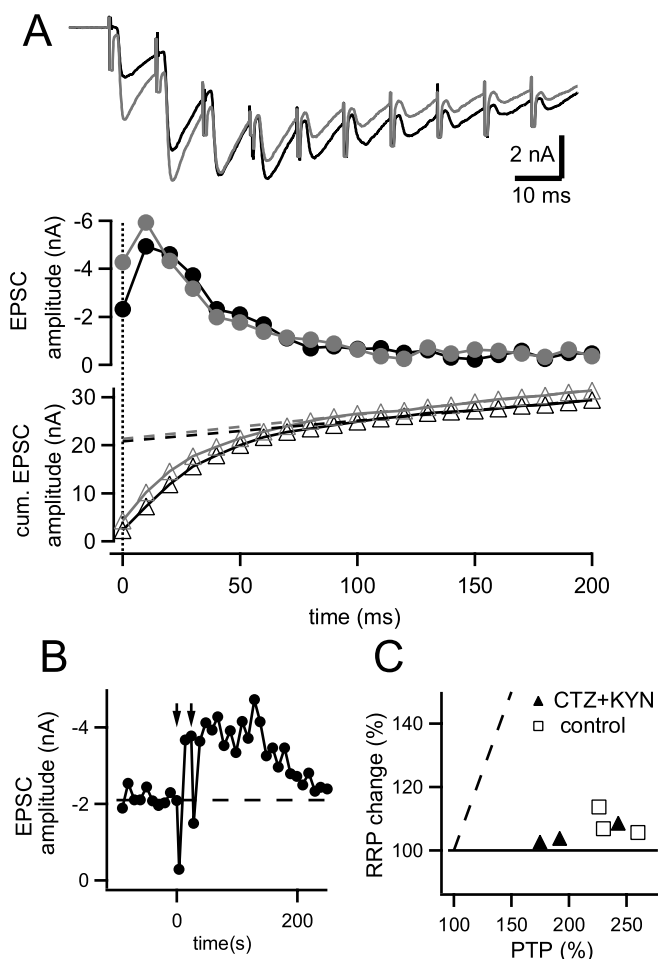


**Figure 4.** The RRP is not significantly increased during PTP. **A**, EPSCs in response to the first 10 stimuli of a 4 s 100 Hz train, both for the first 4 s 100 Hz train, as well as for a second 4 s 100 Hz train applied 20 s later (top; black and gray traces, respectively). The middle panel shows the corresponding plot of EPSC amplitudes for the first 25 stimuli of each 100 Hz train, and the bottom panel shows the plot of cumulative (cum.) EPSC amplitudes, fitted with lines back-extrapolated to time 0 to obtain a measure for the RRP. Black and gray symbols show the results for the first and second 100 Hz trains, respectively. **B**, Time plot of EPSC amplitudes for the experiment illustrated in **A**, with the time of the two 4 s 100 Hz trains indicated by arrows. Note that the first 100 Hz train induced PTP of ~170% of control, but the second 100 Hz train did not increase synaptic strength further. **C**, Plot of the relative pool size increase as a function of the PTP amplitude. The data points for cells with control extracellular solution and in the presence of 1 mM KYN and 0.1 mM CTZ are indicated. The unity line is indicated by the dashed line. The data in this figure were obtained in P4–P6 rats.

receptor desensitization or saturation (Neher and Sakaba, 2001), some of these experiments ( $n = 3$  cells) were done in the presence of 1 mM KYN and 0.1 mM CTZ. However, similar results were obtained in the absence and presence of these drugs (Fig. 4C, open and filled symbols). We conclude that PTP induced by 100 Hz trains is mediated by an increased release probability from an essentially unchanged pool of immediately releasable vesicles.

**PTP is suppressed by EGTA-AM**

To investigate whether PTP at the calyx of Held depends on a presynaptic  $[Ca^{2+}]_i$  increase, we tested whether PTP is sensitive to the membrane-permeable  $Ca^{2+}$  chelator EGTA-AM (Fig. 5). PTP was induced by 100 Hz trains of 4 and 1 s duration applied in an alternating sequence (Fig. 5A). After establishing control PTP for each induction length, 200  $\mu$ M EGTA-AM was applied to the bath. Shortly after the start of EGTA-AM application, the base-

line synaptic strength decreased, and it continued to decrease for >900 s, indicating a slow equilibration of cytoplasmic EGTA concentration. Concomitant with the decrease of baseline synaptic strength, PTP also decreased. This can be seen by comparing PTP under control conditions (Fig. 5B), with PTP induced 27 min after the start of the EGTA-AM application (Fig. 5C).

In these experiments, we analyzed the baseline synaptic strength, which corresponds to the amplitude value  $b$  in Figure 5B, the absolute amount of PTP, which corresponds to the amplitude value  $i$ , and the relative PTP, given by  $(p/b) \times 100$  (Fig. 5B) (see Materials and Methods). Figure 5D plots the average EPSC amplitude and absolute PTP before and during the continuous application of 200  $\mu$ M EGTA-AM ( $n = 6$  cells). Baseline synaptic strength was reduced from a control value of  $4.4 \pm 0.3$  to  $0.7 \pm 0.1$  nA, as analyzed from the baseline EPSC amplitudes averaged from the 10th, 11th, and 12th induction (Fig. 5D, bracket), corresponding to a time of >20 min after the start of EGTA-AM application. The suppression of baseline synaptic strength by EGTA is consistent with previous findings at the calyx of Held (Borst and Sakmann, 1996). In parallel with the decrease in baseline synaptic strength, the absolute PTP decreased, both for 4 and 1 s induction trains (Fig. 5D, open and filled symbols). The relative PTP, plotted in Figure 5E, decreased faster for 1 s induction trains compared with the 4 s trains. This differential onset of the effect of EGTA-AM was probably a consequence of the larger  $Ca^{2+}$  influx caused by the longer induction trains. It is likely that the approximately fourfold larger  $Ca^{2+}$  influx during the 4 s trains saturated the intracellular EGTA, as long as the intracellular concentration of EGTA had not reached a critical value.

In Figure 5F, relative PTP is plotted for control conditions (gray bars) and after application of EGTA-AM for  $n = 4$  cells that were recorded for >30 min after the application of 200  $\mu$ M EGTA-AM. Prolonged bath application of EGTA-AM led to a significant reduction of PTP for both lengths of induction trains ( $p = 0.009$  and  $0.048$  for 1 and 4 s trains) (Fig. 5F). This indicates a role for a (presynaptic)  $[Ca^{2+}]_i$  elevation in PTP.

**Presynaptic  $Ca^{2+}$  requirements for PTP**

We next aimed at imaging presynaptic  $[Ca^{2+}]_i$  during and after the induction of PTP to directly visualize the  $[Ca^{2+}]_i$  signal that might underlie the transmitter release potentiation during PTP. For this purpose, we initially performed presynaptic  $Ca^{2+}$  imaging in simultaneous presynaptic and postsynaptic whole-cell recordings. We found, however, that during presynaptic whole-cell recording, PTP was absent (see below, Fig. 8). We therefore used an alternative  $Ca^{2+}$ -imaging approach, in which calyces were preloaded with fura-4F during a short whole-cell recording (60–120 s), using a pipette solution containing 200  $\mu$ M fura-4F (see Materials and Methods). After removing the presynaptic patch pipette, a whole-cell recording of the postsynaptic cell was made. This allowed us to measure PTP and to image the presynaptic  $[Ca^{2+}]_i$  simultaneously from the fura-4F fluorescence signal arising from the calyx (Fig. 6A).

We imaged  $[Ca^{2+}]_i$  at low sampling rates before and after the 100 Hz train and at higher sampling rate during the 100 Hz induction train (Fig. 6B). In the recording shown in Figure 6, a 100 Hz train of 2 s duration was applied to induce PTP. During the 100 Hz train, presynaptic  $[Ca^{2+}]_i$  rose in a biphasic manner and reached a value of 9.5  $\mu$ M (range, 3–10  $\mu$ M between cells) shortly after the end of the 100 Hz train (Fig. 6B, inset). Thereafter,  $[Ca^{2+}]_i$  dropped to ~300 nM within 0.5 s and then recovered much more slowly (Fig. 6B, arrow). The slowest phase of  $[Ca^{2+}]_i$

recovery can be seen more clearly in Figure 6C, which displays the  $[Ca^{2+}]_i$  signal at a higher gain. The late phase of the  $[Ca^{2+}]_i$  decay was fitted with an exponential function, with a time constant of 32 s in this example (Fig. 6C). In this recording, the baseline synaptic strength was 4.1 nA, and the EPSC amplitude rose to 10.6 nA at the peak of PTP, corresponding to a relative PTP of 260% (Fig. 6D). PTP then decayed with an estimated time constant of 44 s (Fig. 6D).

In these experiments, we also measured the average frequency of mEPSCs before and after PTP induction, with the aim to relate these to the presynaptic  $[Ca^{2+}]_i$ . In the recording of Figure 6, the mEPSC frequency rose to a peak value of 25 Hz in the interval immediately after the 100 Hz train and then returned to baseline values ( $\sim 1$  Hz) with an estimated time constant of 18 s (Fig. 6E). A plot of mEPSC frequency versus  $[Ca^{2+}]_i$  for the time after PTP induction is shown in Figure 6, F and G, on natural and double-logarithmic scales, respectively. There was a good correlation between mEPSC frequency and presynaptic  $[Ca^{2+}]_i$  measured during the slowest phase of the decay of residual  $[Ca^{2+}]_i$  (Fig. 6G), indicating that the increase in mEPSC frequency was driven by presynaptic residual  $[Ca^{2+}]_i$ . The logarithmized data set of Figure 6G was fitted by linear regression, giving a slope of  $1.73 \pm 0.2$  (range, 0.68–2.49;  $n = 9$  measurements in  $n = 5$  cells;  $[Ca^{2+}]_i$  range of 40–270 nM). This slope is significantly lower than the high power relationship of  $\sim 4$ –5, with which  $Ca^{2+}$  regulates transmitter release in a range of 2–8  $\mu M$   $[Ca^{2+}]_i$ , as estimated by  $Ca^{2+}$  uncaging at the calyx of Held (Bollmann et al., 2000; Schneggenburger and Neher, 2000; Felmy et al., 2003). This indicates that elevations of  $[Ca^{2+}]_i$  close to the resting value regulate the rate of transmitter release with a significantly smaller effective  $Ca^{2+}$  cooperativity, in agreement with a recent study at the calyx of Held (Lou et al., 2005).

The  $Ca^{2+}$ -imaging experiments showed that the slowest phase of the decay of residual  $[Ca^{2+}]_i$  has a similar time course as the decay of PTP (Fig. 6C,D), as observed previously at the crayfish neuromuscular junction (Delaney et al., 1989; Delaney and Tank, 1994). Figure 7A plots the decay time constants of PTP and residual  $[Ca^{2+}]_i$  for the entire data set ( $n = 18$  measurements in five cells). Shorter 100 Hz trains, represented by open and light gray symbols in Figure 7A, induced rapidly decaying PTP, whereas longer 100 Hz trains, represented by dark gray and black symbols, tended to induce longer-lasting PTP, in agreement with the results shown in Figure 2C. There was a good correlation between the decay time constant of PTP and the decay time constant of residual  $[Ca^{2+}]_i$  ( $r = 0.81$ ) (Fig. 7A), suggesting that the time course of decay of residual  $[Ca^{2+}]_i$  determines the decay of PTP. Note, however, that most data points were located above the

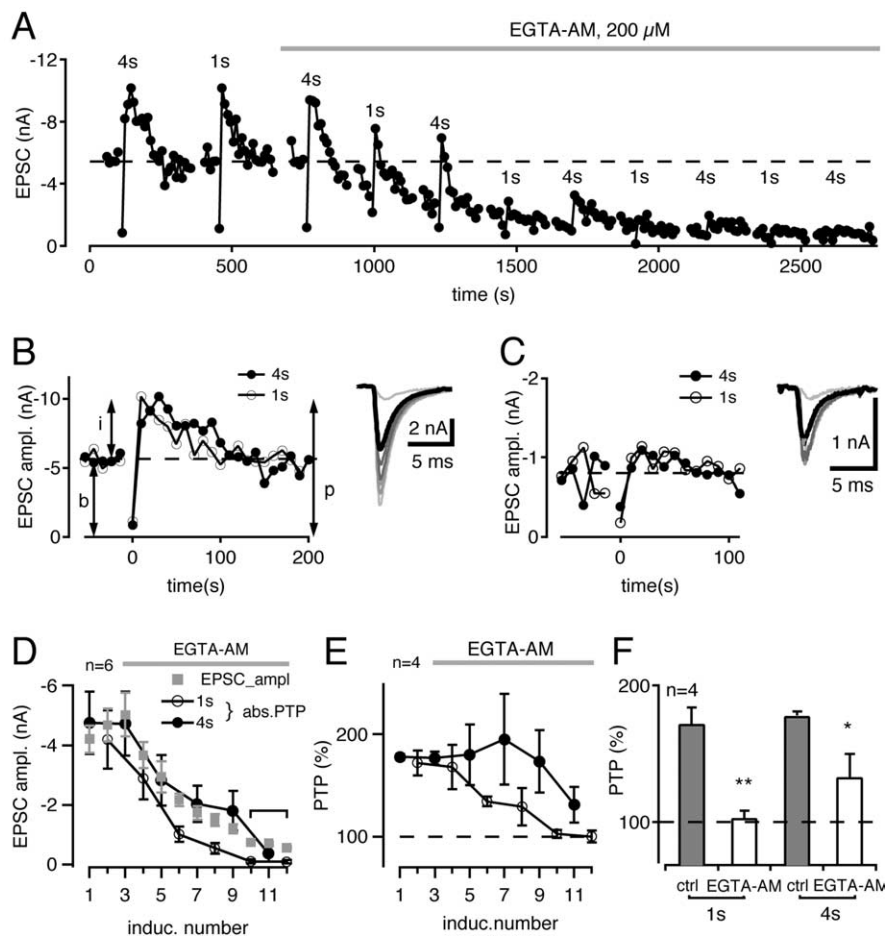


**Figure 5.** PTP and baseline synaptic strength are strongly reduced by the membrane-permeable  $Ca^{2+}$  chelator EGTA-AM. **A**, Plot of EPSC amplitudes versus time in an experiment in which PTP was induced with 100 Hz trains of 1 and 4 s in an alternating sequence. EGTA-AM (200  $\mu M$ ) was applied at the indicated time. **B**, EPSC amplitudes during PTP in response to 1 and 4 s 100 Hz trains under control conditions. The amplitude values *b*, *i*, and *p* were used to calculate absolute and relative PTP in **D** and **E**. The traces on the right show the average EPSC before (black trace) and single EPSCs after (gray traces) PTP induction with a 1 s 100 Hz train. **C**, Same as **B**, but taken 27 min after the onset of the EGTA-AM application. **D**, Time plot of the average EPSC amplitude (gray symbol) and the absolute (abs.) PTP (corresponding to the amplitude value *i* in **B**). Open and filled symbols are absolute PTP for 1 and 4 s induction trains, respectively. The data are from  $n = 6$  cells except the last three data points ( $n = 4$  cells). **E**, Plot of the relative PTP, calculated according to  $(p/b) \times 100$  (see **B**). Open and filled symbols are for 1 and 4 s induction trains, respectively. Average data from  $n = 4$  cells. **F**, Relative PTP in control (ctrl) conditions (gray bars) and after prolonged (> 30 min) application of EGTA-AM (open bars). Asterisks indicate statistical significance ( $*p < 0.05$ ;  $**p < 0.01$ ; paired *t* test). Error bars represent SEM. The data shown in this figure were obtained from P4–P6 rats. ampl., Amplitude; induc., induction.

unity line (Fig. 7A, dotted line). This indicates that on average, the decay of PTP was slightly slower compared with the decay of residual  $[Ca^{2+}]_i$ .

There was also a reasonable good correlation of the decay time constants of mEPSC frequency with the decay time constants of presynaptic residual  $[Ca^{2+}]_i$  (Fig. 7B). In this case, however, the data points fell below the unity line, indicating that decay time constants of the mEPSC frequency tended to be smaller than the decay time constant of the underlying residual  $[Ca^{2+}]_i$ . This is expected if the exponent in the power relationship relating mEPSC frequency to  $[Ca^{2+}]_i$  is somewhat larger than 1, and indeed, this value was 1.73 on average (Fig. 6G).

In Figure 7C, the amplitude of PTP is plotted as a function of residual  $[Ca^{2+}]_i$ , measured at the time when PTP was maximal (at  $\sim 20$ –30 s after the 100 Hz train) (Fig. 6C,D, brackets). It can be seen that robust potentiation of EPSCs of  $\sim 200\%$  is observed for elevations of residual  $[Ca^{2+}]_i$  as low as 40–120 nM over base-

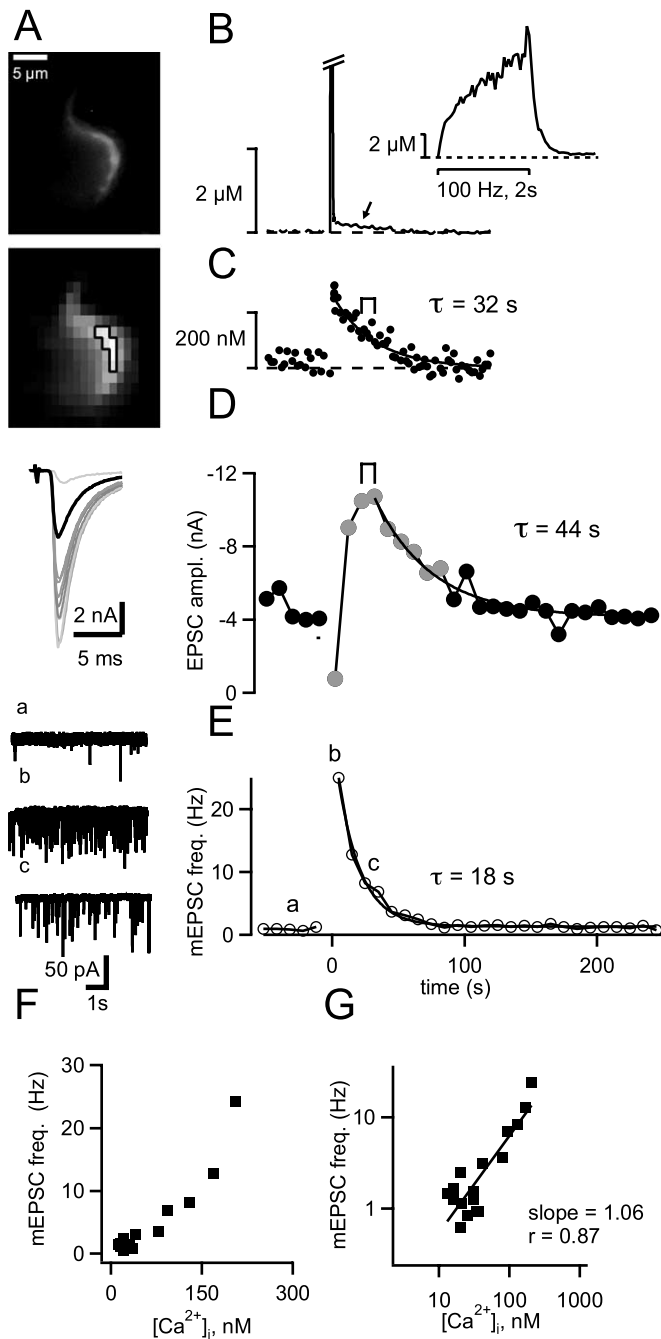


**Figure 6.** Presynaptic  $[Ca^{2+}]_i$  dynamics associated with PTP. The fluorescent  $Ca^{2+}$  indicator fura-4F was preloaded into calyces by a brief whole-cell recording episode. **A**, Fluorescence images taken after the experiment (high resolution; top) and during the experiment (bottom).  $n = 7$  superpixels used for deriving the  $[Ca^{2+}]_i$  traces shown in **B** and **C** are indicated. **B–E**, Time course of  $[Ca^{2+}]_i$  (**B**, **C**), of EPSC amplitudes (ampl.; **D**), and of mEPSC frequency (**E**). At time point 0, a 2 s 100 Hz train was applied. In **B**,  $[Ca^{2+}]_i$  is shown for the entire protocol and for an expanded time during the 100 Hz train (inset). In **C**, the  $[Ca^{2+}]_i$  scale is increased, such that only  $[Ca^{2+}]_i$  up to 350 nM is visible. With this scale, the slowest component of decay of residual  $[Ca^{2+}]_i$  becomes clearly visible, which was fitted by an exponential function with time constant  $\tau = 32$  s. The decay of PTP in **D** was also fitted with an exponential function, giving  $\tau = 44$  s. The time of maximal PTP is indicated by horizontal brackets in **C** and **D**. The traces in **D** show the EPSCs before and after induction of PTP. In **E**, mEPSCs are shown for the time points indicated with a, b, and c in the time plot of **E**. **F**, Plot of mEPSC frequency as a function of presynaptic  $[Ca^{2+}]_i$  during the decaying phase of PTP. **G**, Same data as in **F**, but on double-logarithmic scales. The logarithmized data were fitted with a line, giving a slope of 1.06. freq., Frequency. The data in this figure were obtained from a P5 rat.

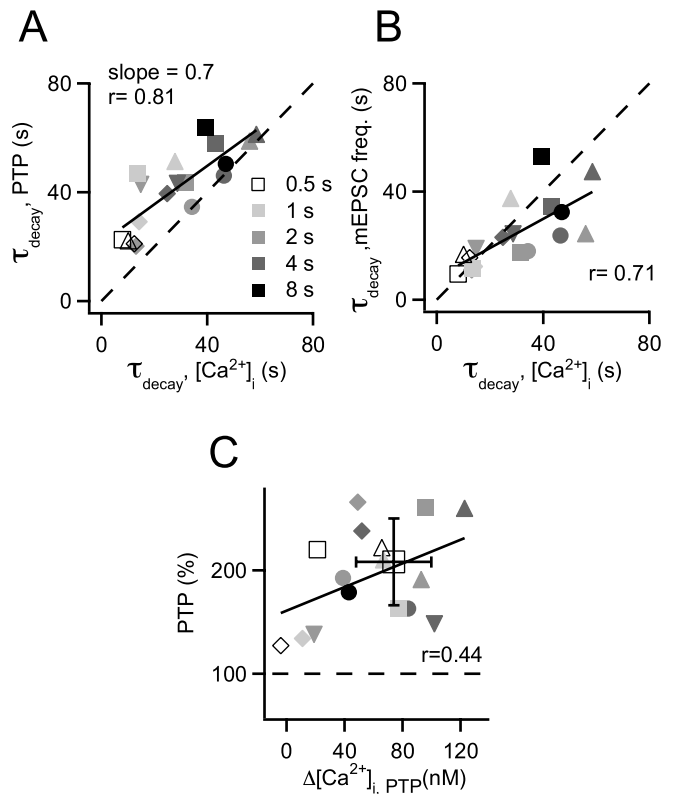


**Figure 7.** The apparent  $Ca^{2+}$  dependence of PTP at the calyx of Held. **A**, Plot of the decay time constants of PTP as a function of the decay time constants of presynaptic residual  $[Ca^{2+}]_i$ . The data points are grayscale coded according to the length of the 100 Hz induction train, as indicated. The data were fitted by linear regression. **B**, Plot of the decay time constant of mEPSC frequency (freq.) as a function of the decay time constant of presynaptic residual  $[Ca^{2+}]_i$ . The data were fitted by linear regression. In **A** and **B**, the dashed line represents the unity line. **C**, Plot of the PTP amplitudes as a function of the presynaptic  $[Ca^{2+}]_i$  at the time of maximal PTP (see Fig. 4C, D, brackets). Linear regression gave a correlation coefficient of  $r = 0.44$ .  $[Ca^{2+}]_i$  is given as the increment over baseline  $[Ca^{2+}]_i$ . The average  $\pm$  SD of all data points  $>40 \mu M \Delta[Ca^{2+}]_i$  are superimposed. The data in this figure were obtained from P4–P6 rats.

line  $[Ca^{2+}]_i$ . The average of the data points  $>40 \text{ nM } [Ca^{2+}]_i$  indicates that for an average  $[Ca^{2+}]_i$  increment of  $74 \pm 26 \text{ nM}$ , PTP was  $208 \pm 42\%$  of control (Fig. 7C, see average  $\pm$  SD data point). Thus, a relatively small elevation of basal  $[Ca^{2+}]_i$  after a high-frequency train induces a robust potentiation of transmitter release during PTP. The correlation between the amplitude of PTP and the increase in residual  $[Ca^{2+}]_i$  in this plot was not strong, however ( $r = 0.44$ ) (Fig. 7C). This might indicate the influence of other factors, such as the control EPSC amplitude, on the amount of PTP (Fig. 3C).

**Whole-cell recording of the presynaptic terminal suppresses PTP**

Finally, we investigated posttetanic potentiation under conditions of presynaptic whole-cell recordings (Fig. 8). We used  $K^+$ -containing presynaptic pipette solutions and recorded the calyces under current-clamp conditions while simultaneously recording from the postsynaptic principal neuron. In the example of Figure 8A, a 4 s 100 Hz induction train was applied twice under conditions of presynaptic whole-cell recording. In both cases, only a slowly recovering phase of synaptic depression was observed, but PTP was absent. This can also be seen in the inset of Figure 8A, which shows presynaptic action potentials and EPSCs before (black traces) and immediately after (gray traces) the 100 Hz

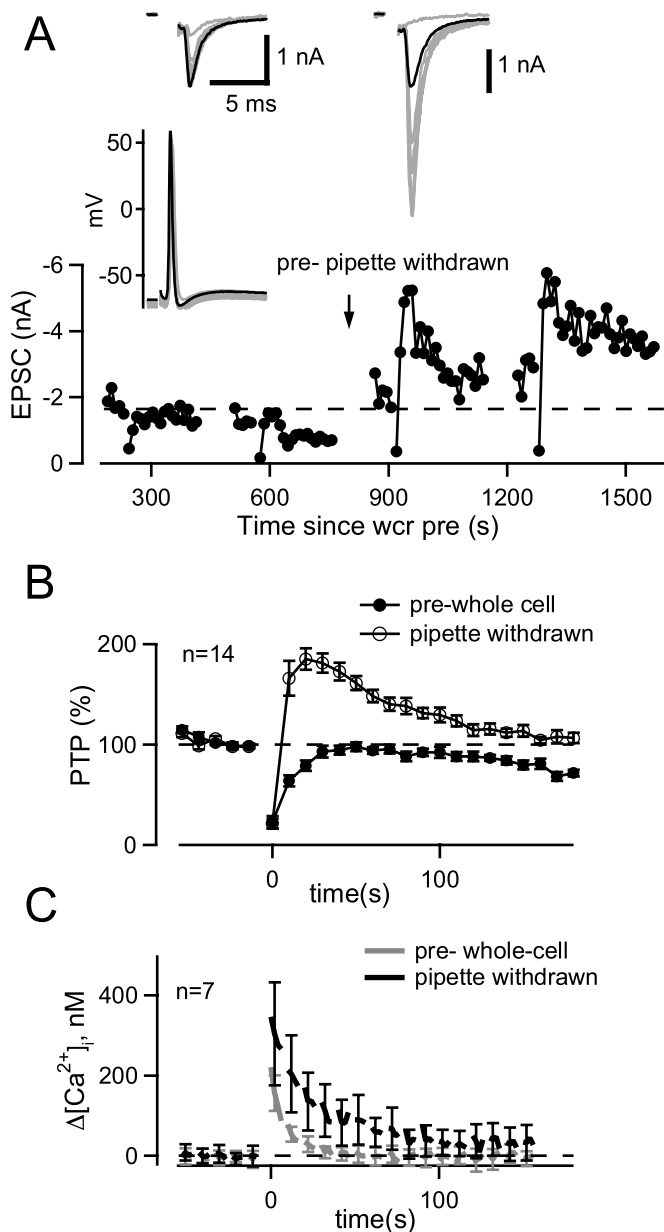


**Figure 8.** Whole-cell recording of the presynaptic nerve terminal reversibly suppresses PTP and accelerates the decay of residual  $[Ca^{2+}]_i$ . **A**, Time plot of EPSC amplitudes. In this experiment, the PTP induction protocol (4 s, 100 Hz train) was given twice under conditions of presynaptic whole-cell recording (wcr pre) and another two times after withdrawal of the presynaptic pipette. The traces on the left show EPSCs and presynaptic APs for control (black traces) and after the induction of PTP (gray traces). The traces on the right show EPSCs for control (black traces) and after the induction of PTP (gray traces), after the presynaptic pipette was removed. **B**, Average time course of relative EPSC amplitude before and after 100 Hz trains of 4 s duration. Filled symbols are under presynaptic whole-cell recording; open symbols are after withdrawal of the presynaptic pipette in the same recordings. **C**, Average residual  $[Ca^{2+}]_i$  measured under conditions of presynaptic whole-cell recording (gray trace) and after pipette removal (black trace) for a subset of cells shown in **B**.  $[Ca^{2+}]_i$  is shown as the increment over the baseline  $[Ca^{2+}]_i$  recorded in each cell. The data in this figure were obtained from P8–P10 rats. Error bars represent SEM.

train. After a recording time of  $\sim 800$  s, the presynaptic patch pipette was withdrawn, and the PTP protocol was repeated twice. In this recording, strong PTP was observed already  $\sim 2$  min after the withdrawal of the presynaptic pipette, and the amount of PTP was stable for the remaining recording period. In other cells, PTP

recovered more gradually after withdrawal of the presynaptic pipette.

In Figure 8B, the average time course of the relative EPSC amplitude is shown for conditions of presynaptic whole-cell recordings (filled symbols) and after removal of the presynaptic patch pipette (open symbols;  $n = 14$  cells; P8–P10). PTP observed after pipette withdrawal was similar to PTP observed in the absence of presynaptic recordings (Figs. 1–3). Thus, PTP reached its peak  $\sim 20$ – $30$  s after the 100 Hz induction train, and the average PTP decayed with a time constant of 57 s (Fig. 8B, open symbols). At the peak of PTP, the average relative PTP was  $183 \pm 10\%$ , similar as in the age-matched control group (Fig. 3B, P8–P10). During presynaptic whole-cell recording, however, the relative EPSC amplitude was only  $86 \pm 5\%$  of control at 20–30 s after the 100 Hz induction train. The difference between the two recording conditions was highly significant ( $p < 0.01$ ; paired *t* test).

The recovery of PTP observed after withdrawal of the presynaptic pipette (Fig. 8A, B) suggests that presynaptic whole-cell recording prevented the build-up of an intracellular signal necessary for PTP, rather than leading to an irreversible loss of intracellular messenger molecule(s) (see Discussion). We therefore tested whether presynaptic whole-cell recording altered the presynaptic  $Ca^{2+}$  signaling. To do so, in a subset of the recordings, we imaged presynaptic  $[Ca^{2+}]_i$  with  $100 \mu M$  fura-4F during presynaptic whole-cell recording and after removal of the presynaptic pipette. The average residual  $[Ca^{2+}]_i$  traces obtained for  $n = 7$  cells are shown in Figure 8C, both under presynaptic whole-cell recording (gray trace) and after pipette withdrawal (black trace). The decay of residual  $[Ca^{2+}]_i$  was significantly faster under conditions of whole-cell recording (time constant,  $9 \pm 2$  s) than after withdrawal of the presynaptic pipette ( $28 \pm 4$  s;  $n = 7$ ;  $p = 0.007$ ; Wilcoxon two-sample test). Under whole-cell conditions, the average decay of residual  $[Ca^{2+}]_i$  was so fast, that at the time of maximal PTP (20–30 s after the induction train), the increment of residual  $[Ca^{2+}]_i$  over baseline  $[Ca^{2+}]_i$  had decayed to only  $25 \pm 15$  nM (Fig. 8C, gray trace). In contrast, after pipette removal, the increment in residual  $[Ca^{2+}]_i$  over baseline  $[Ca^{2+}]_i$  was  $113 \pm 65$  nM (Fig. 8C, black trace). This suggests that during presynaptic whole-cell recordings, PTP was absent because of the faster decay of the residual  $[Ca^{2+}]_i$  signal.

## Discussion

### Identification and developmental regulation of PTP at the calyx of Held

Brief 100 Hz trains of up to a few seconds duration caused robust PTP of synaptic strength at the calyx of Held. The unchanged mEPSC amplitudes during PTP, and the finding that PTP was suppressed by presynaptic whole-cell recording indicates that this transient potentiation of synaptic strength was presynaptic in origin, similar to PTP at other synapses (for review, see Zucker and Regehr, 2002). The decay time constant of PTP depended on the length of the induction train, with time constants in the range of 20–60 s (Fig. 2). This distinguishes this form of synaptic enhancement from augmentation, which decays with a shorter decay time constant ( $\sim 8$  s), independent of the strength of the induction train (Magleby and Zengel, 1976).

Recently, Habets and Borst (2005) showed that prolonged 20 Hz trains induce a longer-lasting form of PTP at the calyx of Held, with decay time constant of  $\sim 9$  min. This form of PTP was associated with an  $\sim 30\%$  increase in the size of the RRP, whereas in our study, the RRP was increased by  $< 10\%$  (Fig. 4). Both studies show that PTP at the calyx of Held is mediated by an increased



release probability without strongly increased RRP, similar to augmentation in hippocampal synapses (Stevens and Wesseling, 1999). It seems possible, though, that during longer-lasting forms of PTP the pool size is increased more substantially (~30%) (Habets and Borst, 2005) compared with the shorter forms of PTP studied here.

We showed that PTP was induced more easily in calyces of Held of young rats (P4–P6) compared with two older age groups studied right before and after the onset of hearing at around P12 in rodents (P8–P10 and P12–P14) (Fig. 3). This adds PTP to a series of functional developmental changes at the calyx of Held, which include the presynaptic AP width, the kinetics of AMPA-receptor-mediated EPSCs, and the amount of synaptic depression (Taschenberger and von Gersdorff, 2000; Iwasaki and Takahashi, 2001; Joshi and Wang, 2002). Together, these developmental changes are thought to help the calyx of Held to reliably transmit trains of high-frequency action potentials. Given the role of presynaptic  $\text{Ca}^{2+}$  in PTP, it is likely that the developmental regulation of PTP is caused by an increased  $\text{Ca}^{2+}$  buffering and  $\text{Ca}^{2+}$  extrusion at the calyx of Held (Chuhma et al., 2001). Indeed, the shift of PTP induction toward longer 100 Hz trains during development (Fig. 3B) was analogous to the effect of EGTA-AM application in young calyces of Held. EGTA-AM blocked PTP induced by weak induction more readily than PTP induced by a stronger induction protocol (1 vs 4 s 100 Hz trains) (Fig. 5E,F). It is thus tempting to speculate that an increase in the expression of an endogenous  $\text{Ca}^{2+}$  buffer with slow binding kinetics, such as parvalbumin (Lee et al., 2000), might contribute to the developmental regulation of PTP. Parvalbumin is expressed at the calyx of Held (Felmy and Schneggenburger, 2004), and its onset of expression at around P8 in rats (Lohmann and Friauf, 1996) coincides well with the downregulation of PTP observed here.

### Presynaptic $\text{Ca}^{2+}$ -dependent mechanism of PTP

Various lines of evidence suggest that PTP is driven by elevations of presynaptic  $[\text{Ca}^{2+}]_i$  in the low nanomolar range (~40–120 nM) (Fig. 7C). First, PTP and the slowest phase of a residual  $[\text{Ca}^{2+}]_i$  signal decayed in parallel with similar time constants, in agreement with previous  $\text{Ca}^{2+}$ -imaging studies (Delaney et al., 1989; Delaney and Tank, 1994; Regehr et al., 1994). Second, PTP was suppressed by the membrane-permeable  $\text{Ca}^{2+}$  chelator EGTA-AM (Fig. 5). Third, whole-cell recording of the calyx of Held reversibly suppressed PTP and accelerated the decay of presynaptic residual  $[\text{Ca}^{2+}]_i$  (Fig. 8). Together, these experiments show that the prolonged presence of residual  $[\text{Ca}^{2+}]_i$  with an increment of ~80 nM over baseline  $[\text{Ca}^{2+}]_i$  is necessary for PTP.

The suppression of PTP by presynaptic whole-cell recordings was probably caused by the accelerated decay of residual  $[\text{Ca}^{2+}]_i$  (Fig. 8C), as opposed to a “wash out” of an intracellular signaling molecule into the patch pipette. This is because PTP readily recovered after removal of the presynaptic pipette (Fig. 8), opposite to what would be expected for an irreversible loss of a diffusible signaling molecule from the cytoplasm. Presynaptic whole-cell recording likely caused a diffusion of  $\text{Ca}^{2+}$ , and possibly also  $\text{Na}^+$ , into the recording patch pipette (Pusch and Neher, 1988) and thereby accelerated the decay of residual  $[\text{Ca}^{2+}]_i$ . Presynaptic  $\text{Na}^+$  accumulation contributes to the residual  $[\text{Ca}^{2+}]_i$  signal by compromising the function of  $\text{Na}^+$ -dependent  $\text{Ca}^{2+}$ -clearance mechanisms (Zhong et al., 2001). Thus, the accelerated decay of the residual  $[\text{Ca}^{2+}]_i$  signal most likely underlies the suppression of PTP during presynaptic whole-cell recording, although it remains possible that presynaptic whole-cell recording

also impaired the function of intracellular signaling pathways, such as the protein-kinase C pathway, which might be involved in PTP (Alle et al., 2001; Brager et al., 2003). In cultured *Aplysia* neurons, PTP was also suppressed by intracellular recordings of the presynaptic neuron, and this effect has also been related to impaired presynaptic  $\text{Ca}^{2+}$  signaling (Eliot et al., 1994).

Given the evidence that PTP is caused by small elevations of presynaptic  $[\text{Ca}^{2+}]_i$  by ~80 nM, how do such small  $[\text{Ca}^{2+}]_i$  elevations increase the transmitter release probability? Considering the estimates of the local  $[\text{Ca}^{2+}]_i$  reached transiently at the  $\text{Ca}^{2+}$  sensor for vesicle fusion (~10–20  $\mu\text{M}$ ) (Bollmann et al., 2000; Schneggenburger and Neher, 2000), it is seen that only a negligible fraction of the overall release potentiation is explained by summation of residual  $[\text{Ca}^{2+}]_i$  with the local  $[\text{Ca}^{2+}]_i$  signal. We would expect a PTP of only 104% of control for a residual  $[\text{Ca}^{2+}]_i$  of 100 nM, assuming a peak local  $[\text{Ca}^{2+}]_i$  of 10  $\mu\text{M}$  and a fourth-power relationship between transmitter release and  $[\text{Ca}^{2+}]_i$ . It is also unlikely that the increased release probability underlying PTP is caused by the same mechanism that causes  $\text{Ca}^{2+}$ -dependent short-term facilitation. It has been shown that brief (~20 ms)  $[\text{Ca}^{2+}]_i$  elevations by ~500–600 nM cause an approximately twofold enhancement of transmitter release during short-term facilitation at the calyx of Held [Felmy et al. (2003), their Fig. 7B]. Thus, the  $[\text{Ca}^{2+}]_i$  increment needed to cause a given enhancement is ~5–10 times higher for facilitation compared with PTP, making it likely that the two forms of short-term plasticity are mediated by different  $\text{Ca}^{2+}$ -dependent mechanisms (Zucker and Regehr, 2002). Short-term facilitation at the calyx of Held has been proposed to result from a mechanism of  $\text{Ca}^{2+}$  summation, aided by supralinearities caused by (partial) saturation of a fast endogenous  $\text{Ca}^{2+}$  buffer (Felmy et al., 2003). However, a mechanism of  $\text{Ca}^{2+}$ -buffer saturation is unlikely to cause significant amounts of PTP, because the small elevation of  $[\text{Ca}^{2+}]_i$  during PTP (~120 nM at most) should not significantly saturate endogenous  $\text{Ca}^{2+}$  buffers. It is possible, though, that the presynaptic mechanism of PTP shares some common properties with the transmitter release potentiation observed after activation of presynaptic glycine receptors at the calyx of Held. Glycine receptor activation leads to subthreshold presynaptic membrane depolarizations, which potentiate transmitter release via an increased presynaptic basal  $[\text{Ca}^{2+}]_i$  (Turecek and Trussell, 2001; Awatramani et al., 2004).

Regarding the role of presynaptic  $\text{Ca}^{2+}$  in PTP, it is useful to consider the mechanism(s) that may underlie the increased transmitter release probability during PTP. First, an enhanced  $\text{Ca}^{2+}$  influx during the presynaptic AP, either as a consequence of AP broadening or by a change in  $\text{Ca}^{2+}$ -channel gating caused by  $\text{Ca}^{2+}$ -channel modulation, could increase the release probability. The fact that we did not observe a change in AP waveform during presynaptic whole-cell recordings (Fig. 8A) does not necessarily argue against AP broadening, because PTP was absent under this experimental condition. Indeed, evidence for a change in presynaptic AP waveform during a longer-lasting form of PTP has been observed recently (Habets and Borst, 2005). Second, a release probability increase could be caused by a transient increase in the  $\text{Ca}^{2+}$  sensitivity of vesicle fusion during PTP.

Together, it is likely that during PTP,  $\text{Ca}^{2+}$  either acts at a high-affinity site relatively tightly associated with the release machinery, but distinct from the low- to intermediate-affinity site that drives vesicle fusion, and causes an increase in the effective  $\text{Ca}^{2+}$  sensitivity of vesicle fusion, in agreement with previous ideas about the action of residual  $\text{Ca}^{2+}$  (for review, see Zucker and Regehr, 2002). Such a high-affinity site could be formed by

Ca<sup>2+</sup>/calmodulin interacting with the presynaptic vesicle priming factor munc-13 (Junge et al., 2004). However, because PTP was not accompanied by a pool size increase, one would have to postulate a postpriming role for munc-13 activated by Ca<sup>2+</sup>/calmodulin. Alternatively, the elevated baseline [Ca<sup>2+</sup>]<sub>i</sub> could activate an intracellular second messenger pathway, such as the protein kinase C pathway implicated in PTP (Alle et al., 2001; Brager et al., 2003), which in turn could increase the Ca<sup>2+</sup> sensitivity of vesicle fusion (Wu and Wu, 2001; Lou et al., 2005) or slightly increase the presynaptic Ca<sup>2+</sup> current (Lou et al., 2005). Future work needs to establish the mechanism of the release probability increase and the modulatory Ca<sup>2+</sup>-binding site(s) involved in the action of Ca<sup>2+</sup> during PTP.

## References

- Alle H, Jonas P, Geiger JRP (2001) PTP and LTP at a hippocampal mossy fiber-interneuron synapse. *Proc Natl Acad Sci USA* 98:14708–14713.
- Awatramani GB, Blackmer T, Trussell LO (2004) Mechanism of enhancement of intra-terminal calcium by weak depolarization in the calyx of Held. *Soc Neurosci Abstr* 30:736.12.
- Bollmann J, Sakmann B, Borst J (2000) Calcium sensitivity of glutamate release in a calyx-type terminal. *Science* 289:953–957.
- Borst JGG, Sakmann B (1996) Calcium influx and transmitter release in a fast CNS synapse. *Nature* 383:431–434.
- Borst JGG, Helmchen F, Sakmann B (1995) Pre- and postsynaptic whole-cell recordings in the medial nucleus of the trapezoid body of the rat. *J Physiol (Lond)* 489:825–840.
- Brager DH, Cai X, Thompson SM (2003) Activity-dependent activation of presynaptic protein kinase C mediates post-tetanic potentiation. *Nat Neurosci* 6:551–552.
- Chuhma N, Ohmori H (1998) Postnatal development of phase-locked high-fidelity synaptic transmission in the medial nucleus of the trapezoid body of the rat. *J Neurosci* 18:512–520.
- Chuhma N, Koyano K, Ohmori H (2001) Synchronisation of neurotransmitter release during postnatal development in a calyceal presynaptic terminal of rat. *J Physiol (Lond)* 530:93–104.
- Clements JD, Bekkers JM (1997) Detection of spontaneous synaptic events with an optimally scaled template. *Biophys J* 73:220–229.
- Delaney KR, Tank DW (1994) A quantitative measurement of the dependence of short-term synaptic enhancement on presynaptic residual calcium. *J Neurosci* 14:5885–5902.
- Delaney KR, Zucker RS, Tank DW (1989) Calcium in motor nerve terminals associated with posttetanic potentiation. *J Neurosci* 9:3558–3567.
- Eliot LS, Kandel ER, Hawkins RD (1994) Modulation of spontaneous transmitter release during depression and posttetanic potentiation of *Aplysia* sensory-motor neuron synapses isolated in culture. *J Neurosci* 14:3280–3292.
- Felmy F, Schneggenburger R (2004) Developmental expression of the Ca<sup>2+</sup>-binding proteins calretinin and parvalbumin at the calyx of Held of rats and mice. *Eur J Neurosci* 20:1473–1482.
- Felmy F, Neher E, Schneggenburger R (2003) Probing the intracellular calcium sensitivity of transmitter release during synaptic facilitation. *Neuron* 37:801–811.
- Forsythe ID, Tsujimoto T, Barnes-Davies M, Cuttle MF, Takahashi T (1998) Inactivation of presynaptic calcium current contributes to synaptic depression at a fast central synapse. *Neuron* 20:797–807.
- Friauf E, Ostwald J (1988) Divergent projections of physiologically characterized rat ventral cochlear nucleus neurons as shown by intra-axonal injection of horseradish peroxidase. *Exp Brain Res* 73:263–284.
- Griffith WH (1990) Voltage-clamp analysis of posttetanic potentiation of the mossy fiber to CA3 synapse in hippocampus. *J Neurophysiol* 63:491–501.
- Gryniewicz G, Poenie M, Tsien R (1985) A new generation of Ca<sup>2+</sup> indicators with greatly improved fluorescence properties. *J Biol Chem* 260:3440–3450.
- Habets RLP, Borst JGG (2005) Post-tetanic potentiation in the rat calyx of Held synapse. *J Physiol (Lond)* 564 1:173–187.
- Hallermann S, Pawlu C, Jonas P, Heckmann M (2003) A large pool of releasable vesicles in a cortical glutamatergic synapse. *Proc Natl Acad Sci USA* 100:8975–8980.
- Harrison JM, Irving R (1966) Ascending connections of the anterior ventral cochlear nucleus in the rat. *J Comp Neurol* 126:51–64.
- Iwasaki S, Takahashi T (2001) Developmental regulation of transmitter release at the calyx of Held in rat auditory brainstem. *J Physiol (Lond)* 534:861–871.
- Joshi I, Wang L-Y (2002) Developmental profiles of glutamate receptors and synaptic transmission at a single synapse in the mouse auditory brainstem. *J Physiol (Lond)* 540:861–873.
- Junge HJ, Rhee J-S, Jahn O, Varoqueaux F, Spiess J, Waxham MN, Rosenmund C, Brose N (2004) Calmodulin and munc13 form a Ca<sup>2+</sup> sensor/effector complex that controls short-term synaptic plasticity. *Cell* 118:389–401.
- Kuwabara N, DiCaprio RA, Zook JM (1991) Afferents to the medial nucleus of the trapezoid body and their collateral projections. *J Comp Neurol* 314:684–706.
- Lee S-H, Schwaller B, Neher E (2000) Kinetics of Ca<sup>2+</sup> binding to parvalbumin in bovine chromaffin cells: implications for [Ca<sup>2+</sup>]<sub>i</sub> transients of neuronal dendrites. *J Physiol (Lond)* 525:419–432.
- Lohmann C, Friauf E (1996) Distribution of the calcium-binding proteins parvalbumin and calretinin in the auditory brainstem of adult and developing rats. *J Comp Neurol* 367:90–109.
- Lou X, Scheuss V, Schneggenburger R (2005) Allosteric modulation of the presynaptic Ca<sup>2+</sup> sensor for vesicle fusion. *Nature*, in press.
- Magleby KL, Zengel JE (1975) A dual effect of repetitive stimulation on post-tetanic potentiation of transmitter release at the frog neuromuscular junction. *J Physiol (Lond)* 245:163–182.
- Magleby KL, Zengel JE (1976) Augmentation: a process that acts to increase transmitter release at the frog neuromuscular junction. *J Physiol (Lond)* 257:449–470.
- McNaughton BL (1982) Long-term synaptic enhancement and short-term potentiation in rat fascia dentata act through different mechanisms. *J Physiol (Lond)* 324:249–262.
- Meyer AC, Neher E, Schneggenburger R (2001) Estimation of quantal size and number of functional active zones at the calyx of Held synapse by nonstationary EPSC variance analysis. *J Neurosci* 21:7889–7900.
- Neher E, Sakaba T (2001) Combining deconvolution and noise analysis for the estimation of transmitter release rates at the calyx of Held. *J Neurosci* 21:444–461.
- Pusch M, Neher E (1988) Rates of diffusional exchange between small cells and a measuring patch pipette. *Pflügers Arch* 411:204–211.
- Regehr WG, Delaney KR, Tank DW (1994) The role of presynaptic calcium in short-term enhancement at the hippocampal mossy fiber synapse. *J Neurosci* 14:523–537.
- Reim K, Mansour M, Varoqueaux F, McMahon HT, Sudhof TC, Brose N, Rosenmund C (2001) Complexins regulate a late step in Ca<sup>2+</sup>-dependent neurotransmitter release. *Cell* 104:71–81.
- Sakaba T, Neher E (2001) Quantitative relationship between transmitter release and calcium current at the calyx of Held synapse. *J Neurosci* 21:462–476.
- Sätzler K, Söhl LF, Bollmann JH, Borst JGG, Frotscher M, Sakmann B, Lübke JH (2002) Three-dimensional reconstruction of a calyx of Held and its postsynaptic principal neuron in the medial nucleus of the trapezoid body. *J Neurosci* 22:10567–10579.
- Scheuss V, Schneggenburger R, Neher E (2002) Separation of presynaptic and postsynaptic contributions to depression by covariance analysis of successive EPSCs at the calyx of Held synapse. *J Neurosci* 22:728–739.
- Schneggenburger R, Neher E (2000) Intracellular calcium dependence of transmitter release rates at a fast central synapse. *Nature* 406:889–893.
- Schneggenburger R, Meyer AC, Neher E (1999) Released fraction and total size of a pool of immediately available transmitter quanta at a calyx synapse. *Neuron* 23:399–409.
- Spirou GA, Brownell WE, Zidnac M (1990) Recordings from cat trapezoid body and HRP labeling of globular bushy cell axons. *J Neurophysiol* 63:1169–1190.
- Stevens CF, Wesseling JF (1999) Augmentation is a potentiation of the exocytotic process. *Neuron* 22:139–146.
- Sun J-Y, Wu L-G (2001) Fast kinetics of exocytosis revealed by simultaneous measurements of presynaptic capacitance and postsynaptic currents at a central synapse. *Neuron* 30:171–182.
- Taschenberger H, von Gersdorff H (2000) Fine-tuning an auditory synapse for speed and fidelity: developmental changes in presynaptic waveform, EPSC kinetics, and synaptic plasticity. *J Neurosci* 20:9162–9173.

- Taschenberger H, Leao RM, Rowland KC, Spirou GA, von Gersdorff H (2002) Optimizing synaptic architecture and efficiency for high-frequency transmission. *Neuron* 36:1127–1143.
- Turecek R, Trussell LO (2001) Presynaptic glycine receptors enhance transmitter release at a mammalian central synapse. *Nature* 411:587–590.
- von Gersdorff H, Schneggenburger R, Weis S, Neher E (1997) Presynaptic depression at a calyx synapse: the small contribution of metabotropic glutamate receptors. *J Neurosci* 17:8137–8146.
- Wang L-Y, Kaczmarek LK (1998) High-frequency firing helps replenish the readily releasable pool of synaptic vesicles. *Nature* 394:384–388.
- Weis S, Schneggenburger R, Neher E (1999) Properties of a model of  $Ca^{++}$ -dependent vesicle pool dynamics and short term synaptic depression. *Biophys J* 77:2418–2429.
- Wong AYC, Graham BP, Billups B, Forsythe ID (2003) Distinguishing between presynaptic and postsynaptic mechanisms of short-term depression during action potential trains. *J Neurosci* 23:4868–4877.
- Wu L-G, Borst JGG (1999) The reduced release probability of releasable vesicles during recovery from short-term synaptic depression. *Neuron* 23:821–832.
- Wu XS, Wu LG (2001) Protein kinase C increases the apparent affinity of the release machinery to  $Ca^{2+}$  by enhancing the release machinery downstream of the  $Ca^{2+}$  sensor. *J Neurosci* 21:7928–7936.
- Zhong N, Beaumont V, Zucker RS (2001) Roles for mitochondrial and reverse mode  $Na^{+}/Ca^{2+}$  exchange and the plasmalemma  $Ca^{2+}$  ATPase in post-tetanic potentiation at crayfish neuromuscular junctions. *J Neurosci* 21:9598–9607.
- Zucker RS, Regehr WG (2002) Short-term synaptic plasticity. *Annu Rev Physiol* 64:355–405.